Published in *Progress in Organic Coatings* (2013) http://dx.doi.org/10.1016/j.porgcoat.2013.05.017

Aesthetically-Textured, Hard Latex Coatings by Fast IR-Assisted Evaporative Lithography

A. Georgiadis, F. N. Muhamad, A. Utgenannt, and J.L. Keddie

Department of Physics, University of Surrey, Guildford, Surrey, GU2 7XH, UK,
j.keddie@surrey.ac.uk

Abstract

Polymer coatings with periodic topographic patterns, repeating over millimetre length scales, can be created from lateral flows in an aqueous dispersion of colloidal particles. The flow is driven by differences in evaporation rate across the wet film surface created by IR radiative heating through a shadow mask. This new process, which we call IR radiation-assisted evaporative lithography (IRAEL), combines IR particle sintering with the concept of evaporative lithography. Here, a series of experiments has been conducted in which the mass of the latex is measured as a function of the exposure time under infrared radiation through a mask. The water evaporation rates and the minimum exposure time required for a dry film are estimated as a function of the power density of the IR emitter. The temperature of the wet film is monitored to avoid overheating and boiling of the water, which will otherwise cause defects. It is demonstrated that textured films can be created on a variety of substrates (plastics, metals, paper and glass), and processing times can be as short as five minutes. We use IRAEL to decorate household goods with an aesthetic coating with the desired texture.

Keywords: patterning, textured coating, latex, infrared radiation, evaporative lithography, infrared sintering

1 Introduction

For numerous applications, there is a need for patterned surfaces at the micro- and nano-length scales. The topography or texture of a surface has a profound influence on its properties. For instance, the correct length scales of surface structure can impart hydrophobicity [1], alter the adhesion [2], reduce the reflectivity of electromagnetic radiation [3], affect friction and wear [4], and reduce the aerodynamic drag on aircraft and hence decrease fuel consumption [5]. There is a variety of techniques with which a patterned polymeric surface can be prepared, including nanopatterning and micropatterning using a mold [6], solution-casting of polymer films [7], photolithography, and inkjet printing. Inspired by previous reports of the evaporative lithography of dilute, hard nanoparticles [8], we recently developed a new technique called infrared radiation-assisted evaporative lithography (IRAEL) [9,10]. This technique introduces a new way to create nearly any-desired pattern of surface topography on a waterborne coating made from a latex dispersion. It is a promising new example of a method that can be classified as "controlled evaporative self-assembly" technique [11].

In IRAEL, a mask containing holes of any desired shape (as in Fig. 1a) is used to modulate the evaporation rate across the surface of a wet colloidal film. The surface tension holds the water surface flat. Water must therefore flow to the fast-drying regions to replenish the water that has been lost by evaporation. This lateral flow carries colloidal particles in the direction towards the unmasked regions (Fig. 1b-c). The result is a collection of particles into a pattern defined by the mask, and these particles coalesce to create a textured coating.

In contrast to the initial work on evaporative lithography, the use of infrared radiation in combination with shadow masks offers two key advantages. First, the heat from the

radiation increases the evaporation rate locally, so that the technique is practical on realistic time-scales. Secondly, polymer particles are sintered by heating from the IR radiation [12], so that patterned coatings can be made from "hard" polymers, with a glass transition temperature far above room temperature.

The use of radiative heating from infrared (IR) sources has gained greater prominence within the past few decades. There are previous reports of the use of IR radiative heating to speed the water loss from waterborne polymers.[13, 14] For instance, the drying time of aqueous solutions of poly(vinyl alcohol) was reduced from 120 min. for convective drying to only 15 min. for combined convective and IR radiative drying.[13] There are also reports of using IR-absorbing polymers as thermal transducers to raise the temperature of hot-melt adhesives[15] and polymer films[16] under IR radiation. IR radiative drying processes are attractive because of their energy efficiency. For example, the energy consumed by an IR lamp combined with a convection oven in removing water from foods was 245% less than that used by the oven alone.[17]

In our previously-reported experiments on IRAEL [9], we used a 250 Watt IR lamp, and textured coatings were created in times on the order of 30 minutes. In the present work, we use a carbon medium-wave emitter, leading to faster film formation times. We determined the effects of the key process parameters of the power of the IR emitter and the distance between the IR emitter and the wet film. (The emitter power and its distance from the film both affect the power density of the IR radiation on the film.) We will show how we can create textured, hard and latex coatings (free of volatile organic compounds, VOCs) in times as short as five minutes.

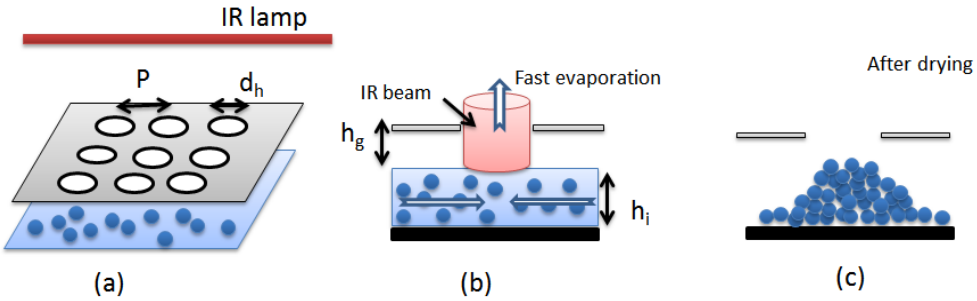

Fig. 1 Overview of the IRAEL process: (a) A colloidal film is placed under a mask. (b) IR radiation heats the wet film in the exposed areas. Particles flow with the water and (c) accumulate under the holes in the mask and sinter as a result of heating. In this figure, the definition of the relevant experimental parameters in IRAEL (h_g, h_i, d_h and P) are provided.

2 Experimental

2.1 Materials

Most of the experiments used a latex made through the semicontinuous emulsion polymerization of methyl methacrylate, butyl acrylate, and methacrylic acid (in a weight ratio of 18.3 : 13.3 : 1), using an ammonium persulfate initiator and an anionic, ethoxylated alcohol surfactant (Rhodafac RK500A, Rhodia). This material is called Latex A hereafter. The glass transition temperature, T_g, of the dry latex, measured by differential scanning calorimetry (Q1000, TA Instruments) at a heating rate of 10 ˚C/min, was 37.9 ˚C. The polymer is glassy at room temperature. The average particle diameter, according to photon correlation spectroscopy (Coulter N4 plus, Beckman-Coulter), was 420 nm. The polymer constituted 52 wt. % of the latex. In experiments to coat glass bottles, a commercially-available acrylic latex (Ucecryl B 30137, provided by Cytec) was used.

IRAEL masks were made from aluminium plates 1.5 mm thick, in which holes with a diameter d_h = 3.5 mm were spaced in an hexagonal array with a fixed centre-to-centre distance, or pitch, P = 5 mm. In most experiments, the films were cast on glass plates (7.5 cm x 5 cm), but in some experiments, the substrates were made from copper, steel, polypropylene, brass, paper and an aluminium alloy.

2.2 Methods

In a typical experiment, a 4 kW carbon IR emitter (Heraeus Noblelight) of length, L = 0.7 m was used. At its maximum power, the emitter has a temperature of 1200 ºC, which corresponds to a peak emission wavelength of 2 μm. This type of emitter has a very fast response time such that it reaches its maximum temperature within 1-2 sec. The emitter was placed at a distance, r, above the wet latex film (Fig. 2a). Textured coatings were made at various values of r and with the power of the emitter, P_E, ranging from 1600 to 2400 W. We can approximate the emission spectrum of the lamp as that of a black body [18]. To provide an indication of the emitter's output, we plot the calculated black body emission for the maximum emitter temperature of 1200 °C and for two lower temperatures for comparison (Fig. 2b). Wien's displacement law [18] tells us that there is an inverse relationship between the wavelength of the peak emission of a blackbody, λ_{max}, and its temperature, T, given as:

$$\lambda_{max} = 2900\ \mu m\ K / T \qquad (1)$$

Thus, the temperature of the emitter can be adjusted so that the peak emission overlaps with the absorbing regions of the substance that is being heated by thermal radiation. Figure 2c shows the temperature dependence of the peak emission. The power density from the carbon IR emitter was measured using an optical power meter (Anritsu, ML910B) with a sensor for the near-IR range between 0.75 μm and 1.8 μm (Anritsu, MA9711A).

As approximately 50 wt.% of a typical latex is water, we are interested in the IR range where there is a strong absorption of water that overlaps with emission of the IR source. Liquid water at 25 ºC has three vibrational modes [19] at 2.93 μm, 4.7 μm and 6.08 μm (Table 1). The strongest one at 2.93 μm is of particular interest here, as it overlaps with the emission of the carbon emitter. Results from the IR emitter are compared to the results obtained with a 250 W near-IR lamp (Model 470 IR, Interhatch). This lamp has a peak emission at a wavelength of 1.2 μm, which is lower than all the main vibrations of water, but the emission extends into the mid-IR range.

The temperature of Latex A films during the IRAEL process was recorded using a digital thermocouple wire attached to the substrate and in contact with the wet latex film. In these experiments, the initial wet film thickness and the initial gap height were kept constant at h_i = 0.65 mm and h_g = 2.05 mm. Evaporation rates of Latex A during the IRAEL film formation process were recorded by placing the wet film on an electronic balance (Sartorius Extend ED2202S-CW) interfaced with a computer to record the data. The balance was shielded from the intense IR radiation by placing insulation on the sample pan. In these experiments, parameter were fixed at h_i = 0.4 mm and h_g = 4.30 mm.

2D contour profiling and 3D mapping were achieved using a stylus profilometer (Dektak 8, Veeco) on the final coatings. Peak-to-valley heights were measured, as described elsewhere [9]. Coatings on flat glass bottles were created by IRAEL under the 4kW IR emitter using the Ucecryl B 30137 latex.

Published in *Progress in Organic Coatings* (2013) http://dx.doi.org/10.1016/j.porgcoat.2013.05.017

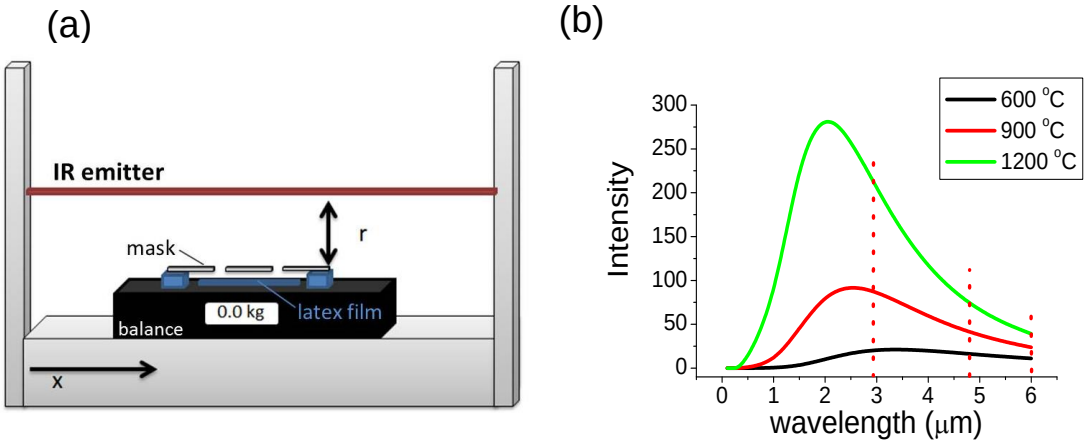

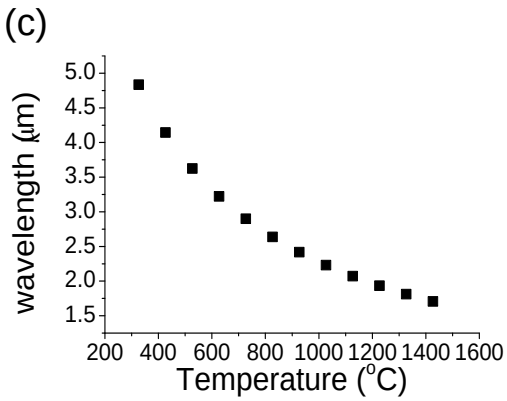

Fig. 2 (a) Schematic diagram of a typical drying experiment. The sample is placed below the mask and both of them are placed on the top of a balance. The IR lamp is placed at distance *r* above the sample. (b) Intensity of lamp radiation emission as a function of the wavelength for different temperatures, as shown in the legend. Vertical lines represent the three main vibrations of liquid water at 25 ºC (c) The wavelength of the *maximum* emittance of a blackbody as a function of its temperature, calculated according to Wien's dispersion law.

Table 1. Three vibrations of liquid water at 25 ºC absorbing in the mid-IR range [19]

Type of Vibration	**Wavelength (μm)**	**Molar Absorptivity (M^{-1} cm^{-1})**
Stretching (asymmetrical + symmetrical) and overtone of bending	2.93	99.9 ± 0.8
Combination of bending and libration	4.7	3.5 ± 0.1
Bending	6.08	21.8 ± 0.3

3 Results

3.1 Characterization of water loss under IR radiation

The heating of a wet latex film, and hence the evaporation, rate, was expected to be a function of the power density, *P*, which is defined as the power of the IR radiation per unit area of film surface. Figure 3 presents readings of the power density when the power of the emitter, P_E, is varied between 0.8 and 4 kW at a distance, *r*, ranging from 5 to 20 cm. At distances of 5 or 8 cm, with the highest power of the emitter (4 kW), the *P* is greater than 1 $W \cdot cm^{-2}$. The figure shows how *P* can be varied between 0 and 1.5 $W \cdot cm^{-2}$ through control of P_E and *r*. The IR emitter offers a tight control of the process conditions for film formation.

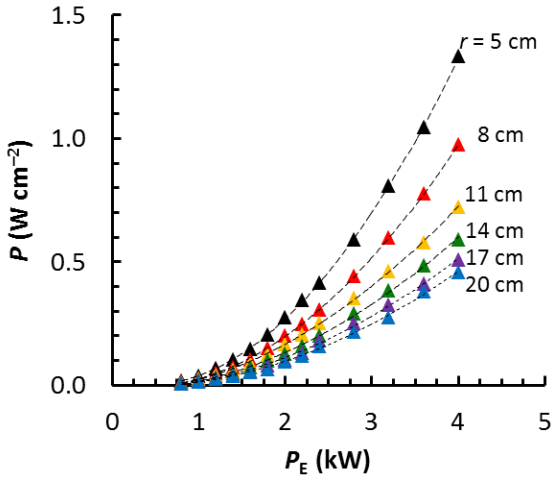

Fig. 3. Power density of IR radiation over a range of distances from the emitter (as indicated) as its power, P_E, is varied.

To characterize the film formation process, we measured the temperature increase in a wet Latex A film during drying under IR radiation from the IR emitter at different power settings, P_E **(Fig. 4).** For this series of experiment, the IR emitter was held above the wet film at a distance of r = 8.8 cm as P_E was varied. Thus, in this experiment, the power density was varied between 0.07 and 0.20 W·cm^{-2}. For all P_E values investigated, the temperature increases at approximately a constant rate. The data show that with a higher power of the IR emitter (P_E = 2200 W), which corresponds to 0.2 W·cm^{-2}, there is a higher rate of temperature increase, such that the boiling point of water (100 °C) is exceeded after four minutes of radiation. Hence, the power density and time must be kept under this limit, because it was found that boiling water led to bubble formation and irregularities in the final textured, hard coating.

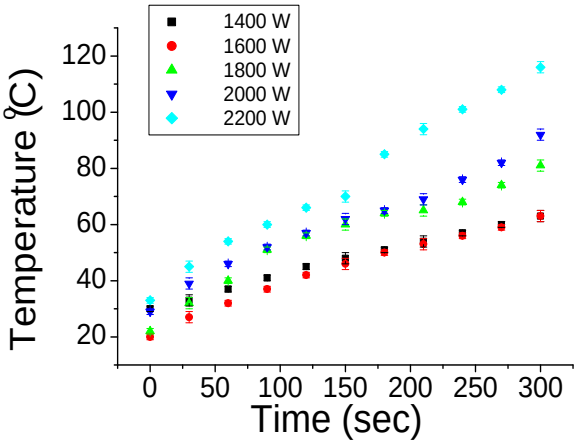

Fig. 4 Temperature as a function of time for different powers of the carbon emitter, P_E, (as indicated by the symbols in the legend) at a fixed distance of r = 8.8 cm. A mask with holes was placed above each sample. These experimental conditions correspond to power densities, P, ranging between 70 mW·cm^{-2} and 200 mW·cm^{-2}.

The power density from a point source varies as the inverse square of the distance, r, from the source, because the area of a surrounding sphere is $4\pi r^2$. In our case, the IR emitter is

cylindrical and not a point source. If L represents the length of emitter, then the power density is expected to vary as

$$P = \frac{P_E}{2\pi r L}. \quad (2)$$

This relation was tested in an experiment where P_E was fixed at 2 kW as r was varied. The data in Figure 5 support an inverse relationship. Equation 2 predicts an energy density of P = 450 mW·cm^{-2} for a distance of r = 10 cm, but the experimental value is lower at 170 mW·cm^{-2}. However, the measurement is not being made over the entire spectrum, and there will be some losses in efficiency such that not all of the emitter's power is converted into IR radiation.

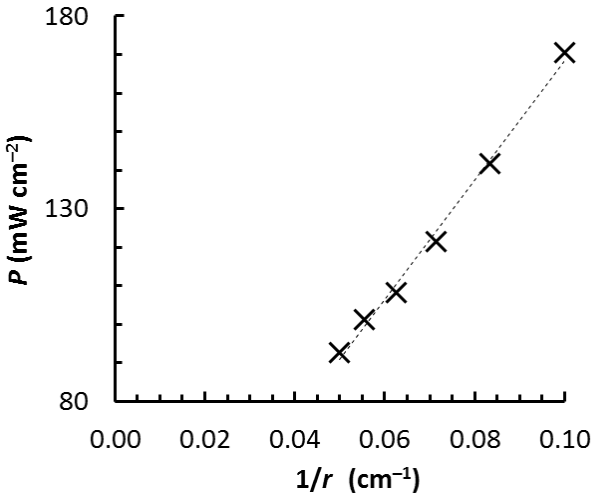

Fig. 5. Inverse relationship between the power density from the IR emitter, P, and the distance from the emitter, r, when the emitter's power is fixed at P_E = 2 kW.

When the film is formed instead under the standard lamp with a power of P_L = 250 W under otherwise identical conditions, the film temperature reaches approximately 70 ºC in 300 s. This rate of heating is close to that obtained when using a power of P_E = 1800 W in the carbon IR emitter. This result might be surprising at first, but it can be explained by considering the power densities. The carbon IR emitter has a higher power than the IR lamp, but it emits along its entire length of L = 0.7 m in a cylindrical area rather than as a point source. When a sample is at distance r, the power density from the emitter and lamp will be equal under this condition:

$$\frac{P_E}{2\pi r L} = \frac{P_L}{4\pi r^2}, \quad (3)$$

where we are making a crude approximation that the lamp is acting as point source emitting over a spherical area. With r = 0.088 m (as used here), the condition defined in Equation 3 will hold when $P_E \approx 4P_L$ = 1000 W, which is on the same order of magnitude found for the emitter power when the two film temperatures are similar. This crude argument does not consider the differences in the distribution of the wavelengths of the emitted radiation. As the carbon IR emitter is at a lower temperature than the lamp, its peak wavelength of emission is at longer wavelengths (by Eq. 1). As the 250 W lamp operates at a higher temperature of 2100 °C, its irradiance (in units of power per unit area of the emitting surface) is *higher than* the 4 kW emitter with a maximum temperature of 1200 °C, as given by the Stefan-Boltzmann

equation [18]. As the precise areas of the emitting surfaces of the two IR sources are not known, a calculation of the total power emitted is not possible. However, the output power density is proportional to the power drawn by the IR sources, as is shown in Figure 3. An obvious advantage of the carbon IR emitter is that its shape allows the processing of coatings by IRAEL along its entire length and hence allows uniform radiation over larger areas compared to the lamp.

In the next series of experiments, we measured the mass of a film as a function of time. A typical result is presented in **Fig. 6**. It is shown here that the mass of the film decreases at a constant rate, until all of the water has evaporated and the mass of the film approaches a constant value equal to the mass of the dried, patterned polymer. From this type of graph, we estimate the evaporation rate from the slope in units of g/s (representing the velocity at which the surface recedes), assuming a density of water of 1 g cm^{-3}, and using the measured area of the coating (in units of cm^2). There is an inflection point at which the rate of mass loss approaches zero, and it defines the time to dry, t_{dry}. This second parameter is very important from a practical point of view, as we can use it to estimate how long is needed to expose the coating to the infrared radiation to remove the water.

We have observed, however, if the IRAEL process is stopped immediately after t_{dry}, the coating is dry but turbid because of light scattering from intra-particle voids. This result occurs when the latex particle sintering time is longer than the drying time of the film. The film formation process is shifted to a dry sintering regime.[20,21] Upon continued exposure to IR radiation, the dry particles coalesce, driven by the reduction of the surface energy of the polymer/air interface.[12] When the interparticle voids are closed, the coating becomes optically transparent.

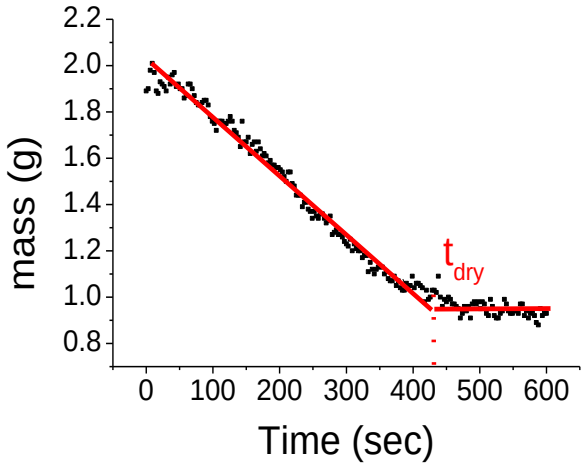

Fig. 6. An example of the mass loss from a wet Latex A film under IR irradiation. From this type of graph, the evaporation rate is calculated from the gradient, and the time to dry, t_{dry}, is found from the inflection point, as shown.

The evaporation rates have been measured as a function of the power of the emitter **(Fig. 7)**. For this series of experiments, the distance from the lamp was fixed at r = 14.5 cm, and the power densities ranged from 69 to 265 mW·cm^{-2} (see Table 2). The experiment was conducted by two methods. In the first method, the mask was used, whereas in the second, no mask was used. From these results, it can be seen that a higher power of the IR emitter leads to higher evaporation rates. With or without the mask, the evaporation rate shows a similar linear dependence on the emitter's power. Without the mask, an evaporation rate of 1.5×10^{-4} cm s^{-1} is achieved, which is more than 20 times greater than what is found under static air at

room temperature (7×10^{-6} cm s^{-1}) [22]. Furthermore, this value is near the maximum value of 2.0 x 10^{-4} cm s^{-1} reported elsewhere[23] for water evaporation under medium-wave (2 – 2.8 μm) IR radiation. The use of the mask leads to an evaporation rate that is approximately one-third lower than for the uncovered surface. The mask covers one-third of the surface area of the coating (with holes over the remaining two-thirds). Hence, the reduction in the evaporation rate is easily explained by the blocking of the surface by the mask.

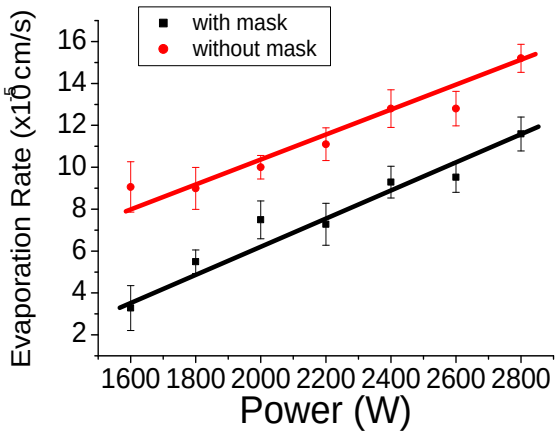

Fig. 7. Evaporation rates of Latex A as a function of power of the carbon emitter, P_E, with (black squares) and without (red circles) a mask covering the wet film, with the lamp fixed at a distance of r = 14.5 cm. As the power of the emitter is varied from 1600 to 2800 W, the power density varies from 69 to 264 mW·cm^{-2}.

Table 2. Power densities at three distances from the IR emitter with a range of powers

	Power Density (mW·cm^{-2})		
	Distance, *r* (cm)		
P_E (kW)	**12**	**14.5**	**16**
1.6	77.9 ± 2.7	69.1 ± 1.6	65.9 ± 1.3
1.8	113.7 ± 2.4	94.6 ± 1.6	89.13 ± 0.9
2.0	151.6 ± 2.9	121.0 ± 1.5	116.8 ± 1.9
2.2	194.6 ± 3.3	150.1 ± 1.6	145.8 ± 1.6
2.4	235.5 ± 4.6	185.2 ± 2.6	168.6 ± 1.4
2.6	283.2 ± 1.8	225.8 ± 2.1	204.1 ± 1.3
2.8	323.1 ± 4.7	264.5 ± 0.6	231.7 ± 5.9

The dependence of the drying times on the IR emitter power (and thus the power density) was explored in experiments. Fig. 8 shows results for two distances: r =12 cm and r =16 cm. (The corresponding power densities are listed in Table 2.) It is seen in the figure that both higher P_E and smaller r lead to shorter drying times. At a power of P_E = 2400 W and a distance of r = 12 cm, which results in a power density of 236 mW·cm^{-2}, the textured coatings dry in five minutes. At higher P_E or shorter distances, boiling of the water negatively affects the film quality. When r is smaller, the power density and hence the evaporation rate is higher.

One would expect that as evaporation rate is proportional to the IR power density, and as the power density for a cylindrical lamp varies as r^{-1} (as was presented in Fig. 5), the evaporation rate should similarly be proportional to r^{-1}. Fig. 9 shows that this relationship is

not exactly followed, probably because the assumptions are not strictly true. However, the evaporation rates are lower when the lamp is farther away, as is expected.

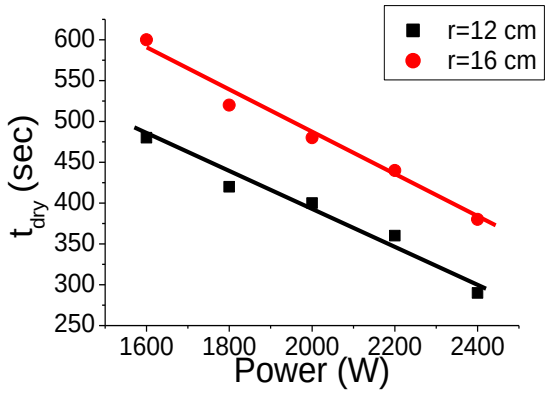

Fig. 8. Drying times as a function of power of the carbon IR emitter, P_E, for r = 12 cm (black squares) and r = 16 cm (red circles) with a mask over the Latex A coating.

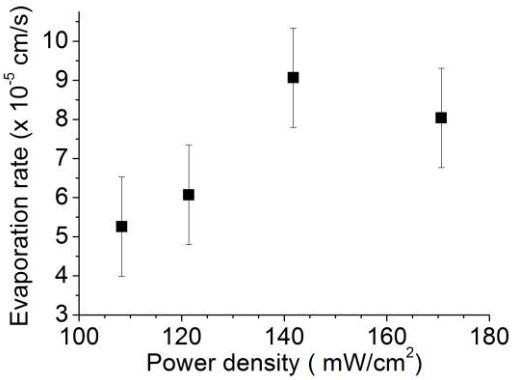

Fig. 9. Dependence of the evaporation rate on the power density, measured when the distance between the emitter and the film were varied with a fixed emitter power of P_E = 2000 W.

3.2 Characterizing IRAEL of textured coatings

Harris *et al.* [8] argued that in standard evaporative lithography there is a flux of water laterally in the plane of the coating which replaces the water lost from the evaporating regions and carries the particles. They derived an equation to relate the horizontal velocity of the particles to the evaporation rate. As the evaporation rate was found in the present work to increase with the power of the IR emitter, P_E, the horizontal particle velocities are likewise expected to increase with P_E. A series of experiments was conducted to determine whether P_E affected the surface topography.

IRAEL was used to create a series of textured coatings, using a range of P_E values going from 800 W to 2400 W. The mean peak-to-valley height, *PV*, of the topography of each coating was measured as a means of characterizing the topography. There was not a significant variation in *PV* across the range of emitter powers. We interpret this finding by suggesting that faster particle velocities (driven by faster evaporation rates) in our system do not result in a greater accumulation of particles. The particles merely arrive at their final destination faster. However, in cases in which transport by particle diffusion is important [8],

such that it opposes the flow to the fast-evaporating regions, then the particle velocity - driven by evaporation - is expected to influence the surface topography.

3.3 Creation of aesthetic textured coatings

One purpose of these experiments was to optimise the IRAEL process and to determine the experimental parameters that will allow the technique to be adopted in the industrial sector. One possible target is to use the patterning technique to decorate household goods. Additional experiments have been conducted to determine the limits of the technique. Replacement of the circular holes in the metallic masks with square, triangles and rectangular holes resulted in films with square, triangle, and rectangular features. Furthermore, the process has been applied to a variety of substrates including glass, copper, steel, aluminium, brass, polyester and paper. It was found that the IRAEL process was successful on each of the substrates. Table 3 shows that the peak-to-valley heights of the surface texture for the different substrates under the same conditions vary by about a factor of four from paper (56.9 μm) to glass (252.7 μm). We believe that the differences in the observed values are due to the combined effects of different thermal conductivities, IR absorptions, and surface energies of the various substrates. However, it is difficult to fully explain this trend. Further experiments and simulations are needed to understand it.

Table 3. Peak-to-valley heights of the features in patterned latex films on different substrates

Substrate	**Peak-to-valley height (μm)**
Brass	229.9 ± 14.0
Copper	232.6 ± 14.2
Steel	198.5 ± 16.5
Glass	252.7 ± 13.3
Paper	56.9 ± 14.1
Aluminium Alloy	190.0 ± 10.6
Polyester	166.7 ± 24.4

To assist the scale-up of the process, we investigated the maximum area over which a single IR emitter could be used to apply textured coatings. The objective is to coat several objects in a batch process. For this purpose, the coated substrates were positioned horizontally below the IR emitter at different positions along the *x* direction (see Fig. 2a). A total of seven glass substrates (with a Latex A coating) were placed (not simultaneously) at different positions, *x*, spaced along the full length of the emitter. We observed that, in all cases, the patterns were similar and well defined. Hence, batch processing is possible when using the 0.7 m emitter.

Finally, we demonstrated that the patterning of three-dimensional objects with a commercial acrylic latex (Ucecryl B 30137) is possible via IRAEL using the 4 kW emitter. Fig. 10 shows bottles with textured coatings that were processed in approximately eight minutes. As the polymer is well below its glass transition temperature at room temperature, the coating is hard. The coating provides an attractive and distinctive appearance to the objects.

Although this present work has considered applications in coatings, the assembly of nanoparticles over large areas provides a means of creating metamaterials with desired optical and electronic properties [24]. Furthermore, IRAEL can be applied to blends of inorganic and organic particles [25] to create hierarchically-structured nanocomposites with nanoparticles periodically arranged over large distances [26, 27]. Such materials promise useful optical,

electrical and mechanical properties, and achieving control over particle assembly in a continuous polymer matrix remains a challenge [28], which can potentially be met by IRAEL.

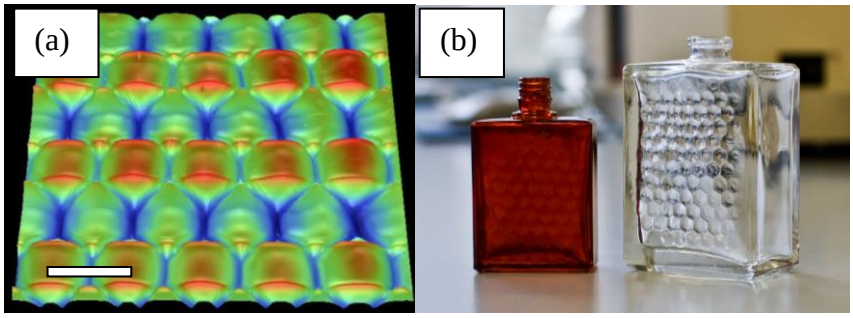

Fig. 10 mW·cm^{-2} (a) A topographic 3-D image of a patterned coating made by IRAEL using an acrylic copolymer dispersion (Ucecryl B 30137). In this experiment, the pitch, P = 5 mm, the gap between the film and mask, h_g = 1 mm, and the film thickness, h_i = 0.4 mm. Scale bar is 5 mm. (b) Flat bottles decorated with aesthetic textured coatings via IRAEL processing.

4 Conclusions

A new, simple and inexpensive patterning technique has been developed. With this technique, called IRAEL, a variety of textures with a range of heights and pitches can be achieved. Because film formation occurs under the IR heating, there is no need for plasticizers for hard polymers and hence no emission of organic compounds during film formation.

Higher powers and smaller distances between the lamp and film both lead to higher evaporation rates and shorter drying times. The power density irradiating the coating surface, which is a function of the power and the distance away, is a key parameter in controlling the rate of the IRAEL process. With an IR emitter power of 2400 W and a distance of 12 cm to the wet film (resulting in a power density of 235 mW·cm^{-2}), a dry coating is obtained within five minutes. The presence of the mask decreases the evaporation rate from the latex in approximate proportion to the area of the surface that is covered. Higher power densities overheat the wet film, causing it to boil and leading to poor coating quality.

The IRAEL process was used to create novel, textured waterborne coatings to decorate glass bottles. The process can be applied on nearly any substrate, and it is suitable for batch processing. Hard waterborne coatings can be created without the use of VOCs or volatile plasticizers.

Acknowledgements

This work was funded the EPSRC Knowledge Transfer Account (KTA) at the University of Surrey. A.G. acknowledges a previous Ph.D. studentship from the UK Engineering and Physical Sciences Research Council (EPSRC) and Akzo Nobel. We benefitted from useful discussions with Martin Murray, Phil Beharrell and John Jennings (all at Akzo Nobel); Keltoum Ouzineb and Elodie Siband (Cytec Surface Specialties); Jon Wood (Heraeus Noblelight Ltd). We are grateful to Tim De Rydt (Akzo Nobel) for providing glass bottles. Violeta Doukova (University of Surrey) provided laboratory assistance.

References

[1] S. M. Lee, T. H. Kwon, Nanotechnology 17 (2006) 3189-3196
[2] C. Poulard, F. Restagno, R. Weil, L. Leger, Soft Matter 7 (2011) 2543-2551
[3] J. Lekner, Theory of Reflection: Of Electromagnetic and Particle Waves, Springer, Dordrecht, Netherlands, 1987, Ch. 11
[4] U. Pettersson, S. Jacobson, Tribol. Int. 36 (2003) 857-864
[5] R. Grüneberger, W. Hage, Experiments in Fluids, 50 (2011) 363-373
[6] S. H. Kim, J. H. Jeong, J. R. Youn, Nanotechnology 21 (2010) 205302
[7] M. Srinivasarao, D. Collings, A. Philips, S. Patel, Science 292 (2001) 79-83
[8] D. J. Harris, H. Hu, J. C. Conrad, J. A. Lewis, Physical Review Letters 98 (2007) 148301
[9] A. Georgiadis, A. F. Routh, M. W. Murray, J. L. Keddie, Soft Matter 7 (2011) 11098-11102
[10] J.L. Keddie and A. Georgiadis, international patent application (2011) WO2011-051648
[11] W. Han and Z. Lin, Angew. Chem. Int. Ed., 51 (2012) 1534-1546
[12] A. Georgiadis, P. A. Bryant, M. Murray, P. Beharrell, J. L. Keddie, Langmuir 27 (2011) 2176-2180
[13] N. Salagnac, P. Glouannec, Heat and Mass Transfer 43 (2007) 177-182
[14] J. Kajtna, U. Sebenik, M. Krajnc, J. Golob, Drying Technology, 26 (2008) 323-333.
[15] F. Li, M.A. Winnik, A. Matvienko, A. Mandelis, J. Mater. Chem., 17 (2007) 4309-4315
[16] H.E. Cingil, J.A. Balmer, S.P. Armes, P.S. Pain, Polymer Chemistry, 1 (2010) 1323-1331
[17] K. Krishnamurthy, H.K. Khurana, S. Jun, Comp. Rev. Food Sci. & Food Safety, 7 (2008) 2-13
[18] H. Ohanian, Physics, 2nd edition expanded, Norton, 1989, pp. 1027-1033
[19] S. Y. Venyaminov, F. G. Prendergast, Analytical Biochemistry 248 (1997) 234-245
[20] A.F. Routh, W.B. Russel, Langmuir 15 (1999) 7762-7773
[21] W.B. Russel, N. Wu, W. Man, Langmuir 24 (2009) 1721-1730
[22] P. Ekanayake, P.J. McDonald, J.L. Keddie, European Physical Journal – Special Topics 166 (2009) 21-27
[23] M.A. Rösler, E. Klinke, G. Kunz, Prog. Organ. Coat. 23 (1994) 351-362
[24] K. J. Stebe, E. Lewandowski, and M. Ghosh, Science, 325 (2009) 159-160
[25] H. Luo, C.M. Cardinal, L.E. Scriven, and L.F. Francis, Langmuir 24 (2008) 24, 5552-5561.
[26] D. J. Harris, J. C. Conrad, and J. A. Lewis, Phil. Trans. Ser. A, 367 (2009) 5157-5165
[27] A. Utgenannt, J.L. Keddie, O.L. Muskens and A.G. Kanaras, Chem. Comm. (2013), to appear.
[28] A.C. Balazs, T. Emrick, and T.P. Russell, Science 17 (2006) 1107-1110.

Highlights

- A new, simple and inexpensive patterning technique has been developed.
- This process combines IR particle sintering with the concept of evaporative lithography.
- Under optimised conditions a hard textured coating can be obtained within five minutes without the addition of volatile organic compounds, such as coalescing aids.
- The process was used to create novel, textured waterborne coatings to decorate glass bottles.
- The process can be applied on nearly any substrate, and it is suitable for batch processing.

Published in *Progress in Organic Coatings* (2013) http://dx.doi.org/10.1016/j.porgcoat.2013.05.017

Table of Contents Image